

ratio $p_1/p_2=4$ in the range $2 \div 5 \times 10^{-15}$ sec of mean life, as well as with the assumption of associated charmed meson baryon photoproduction.

The cross section corresponding to these two trident-like events is $\sim 0.5 \mu b$.

Alternatively, if we disregard such events and if we assume the theoretically expected value for the lifetime to be right, say 7×10^{-13} sec,⁸ then we conclude from our data (see Fig. 2) that the charm photoproduction cross-section must be lower than $1 \mu b$.

References

1. CERN/SPSC/74-29; SPSC/P-10, April 1974.

2. CERN/SPSC/76-13; SPSC/P78/Add 2, 13 December 1977.
3. CERN/SPSC/76-17/P-10 Add 1, 19 February 1976.
4. F. Bleezacker *et al.*: report UCSB TH-18, 1976.
5. W. Lee: *Proc. Int. Symp. Lepton and Photon Interactions at High Energies*, (Hamburg, 1977) p. 555.
6. B. Margolis: *Phys. Rev. D17* (1978) 1310.
7. CERN/EP/PHYS 72-25, 26 July 1978 and Beam Dump Gargamelle Collaboration: submitted to the Topical Conference on Neutrino Physics, Oxford, 2-7 July 1978.
8. N. Cabibbo *et al.*: PAR-LPTHE 78/12, June 1978.

PROC. 19th INT. CONF. HIGH ENERGY PHYSICS
TOKYO, 1978

B 4 Photoproduction at the SPS- ϕ , ρ' , $K^+K^-\pi^+\pi^-$ and a Search for Charmed Mesons

Presented by A. KEMP

Bonn, CERN, Ecole Polytechnique, Glasgow, Lancaster, Manchester, Orsay,
Paris LPNHE, Rutherford, Sheffield Collaboration

This paper presents some of the first results from the Omega Tagged Photon Collaboration at the CERN SPS. The physics topics are:

- 1) $\gamma p \rightarrow \phi p$
- 2) $\gamma p \rightarrow \rho'(1500)p$
 $\downarrow \pi^+\pi^-\pi^+\pi^-$
- 3) $\gamma p \rightarrow K^+K^-\pi^+\pi^-$
- 4) $\gamma p \rightarrow$ Charmed mesons

The experimental arrangement for these measurements is shown in Fig. 1.

The tagged photon beam was produced from an 80 GeV tertiary electron beam from the SPS. The photons were directed at a 670 mm liquid hydrogen target situated in the Omega magnetic field; the mean field was 0.9 tesla. Photoproduced particles were detected by spark chambers and wire proportional chambers inside the magnetic field region and by drift chambers at the downstream end of the magnet. A 32-cell Cerenkov counter, placed downstream of the drift chambers as shown in Fig. 1, was used to identify K^\pm and

p^\pm . A large lead-glass array was used to detect γ -rays; the results of measurements involving π^0 's will be reported at a later date.

1. Elastic ϕ production

The trigger for process (1) required two or three charged prongs with the requirement that at least one track passed through the Cerenkov and was below the threshold which was 5 GeV/c for π^\pm , 17 GeV/c for K^\pm and 34 GeV/c for p^\pm . Consequently the data is restricted to the range $20 \text{ GeV} < E_\gamma < 35 \text{ GeV}$. The t -distribution of events in the ϕ peak is given by:

$$d\sigma/dt \cdot BR = ae^{bt}$$

with

$$a = (1.18 \pm 0.15) \text{ nb GeV}^{-2}$$

$$b = (5.5 \pm 1.2) \text{ GeV}^{-2}.$$

Thus $\sigma(\gamma p \rightarrow \phi p) \cdot BR(\phi \rightarrow K^+K^-) = 215 \pm 13 \text{ nb}$ (± 39 nb systematic error)

The resulting value $\sigma(\gamma p \rightarrow \phi p) = 442 \pm 29 \text{ nb}$ agrees well with the results from the Santa Barbara-Toronto-Fermilab group.

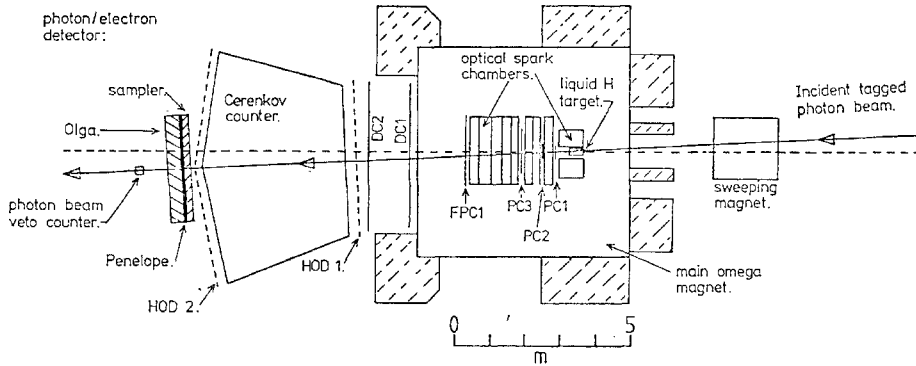


Fig. 1.

2. $\rho'(1500)$

The trigger requirement was ≥ 4 particles leaving the target volume and reaching PC3 (Fig. 1). Reaction (2) was selected by the requirement that $|E_\gamma - \sum E_\pi| < 1$ GeV; where E_γ and E_π are the energies of the incoming photon and outgoing pions respectively.

The 4π invariant mass distribution is shown in Fig. 2. Production is peripheral (αe^{bt}) with a slope parameter $b = 5.1 \pm 0.2$ GeV $^{-2}$ for $M(4\pi) < 1.7$ GeV. In contrast to peripheral phase space, which peaks at a mass ~ 3.5 GeV/c 2 , the data show a broad enhancement centred at 1.5 GeV/c 2 , FWHM ~ 0.5 GeV/c 2 . We identify this with $\rho'(1500)$ seen by other authors. The $\pi^+ \pi^-$ mass distribution shows a strong $\rho(770)$ signal, $\sim 1/2 \rho$ per event. There is no evidence for $\rho^0 \rho^0$ decay, as expected if $C = -1$. A maximum likelihood fit shows that $J^p = 1^-$ decaying to $\rho \pi^+ \pi^-$ dominates, as shown by Fig. 2.

3. $\gamma p \rightarrow K^+ K^- \pi^+ \pi^-$

This channel is of interest since high mass vector mesons, in particular recurrences of the ϕ , are expected to decay into $K^* K \pi$. Events were selected to have topology compatible with channel (3), having two tracks identified as K 's (momenta 5–17 GeV/c) by the Cerenkov counter, and by requiring that $|E_\gamma - E_\pi| < 1.5$ GeV. We estimate a channel cross section of 75^{+50}_{-25} nb. From a study of events with a recoil proton we estimate the contamination from $\bar{p} p \pi^+ \pi^-$ to be $\sim 25\%$.

The $K^+ K^- \pi^+ \pi^-$ mass distribution is shown in Fig. 3a. In contrast to the expectation from peripheral phase space (solid line), a broad threshold enhancement is present. The shaded histogram in Fig. 3a shows that there is a significant $K^* K \pi$ content whereas Fig. 3b shows no enhancement for $\phi \pi^+ \pi^-$. There is no evidence for the decay $K^* \bar{K}^*$. The momentum transfer distribution (not shown) is peripheral

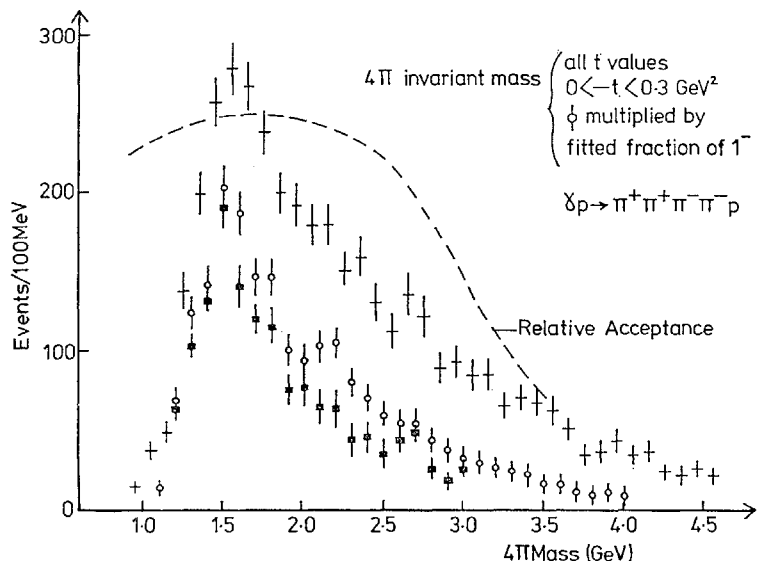


Fig. 2.

with a slope $\sim 5 \text{ GeV}^{-2}$ for $M(KK\pi\pi) < 2 \text{ GeV}/c^2$.

In summary, the data show a peripherally produced threshold enhancement that decays to $KK\pi\pi$ and $K^*K\pi$, but not to $\phi\pi\pi$. We remark on the similarity to the ρ' seen in $\gamma p \rightarrow p\pi^+\pi^+\pi^-\pi^-$.

4. $\gamma p \rightarrow \text{charmed mesons}$

The trigger requirement in this case was a multiplicity ≥ 4 and at least one track $\geq 5 \text{ GeV}/c$ which did not fire the Cerenkov. Events for the present analysis were further selected off-line by a more precise test of the Cerenkov requirement. Data were also recorded which did not have to satisfy the Cerenkov requirement and these will be the subject of a separate analysis, including K^0 and Λ^0 , at a later date.

The acceptance for inclusive D -meson production was obtained from a Monte Carlo simulation which took into account the trigger requirements and off-line cuts. The acceptance is approximately 0.4 for all values of $x = p_L/p_{L,\max}$ greater than zero and for $p_T < 1.0 \text{ GeV}/c$.

The mass resolution was estimated from simulated data and from fitting the $K^*(890)$

data in the $K\pi$ channels. The fits give a resolution at the K^* mass of 38 MeV (FWHM); this scales to 76 MeV at the D mass, assuming

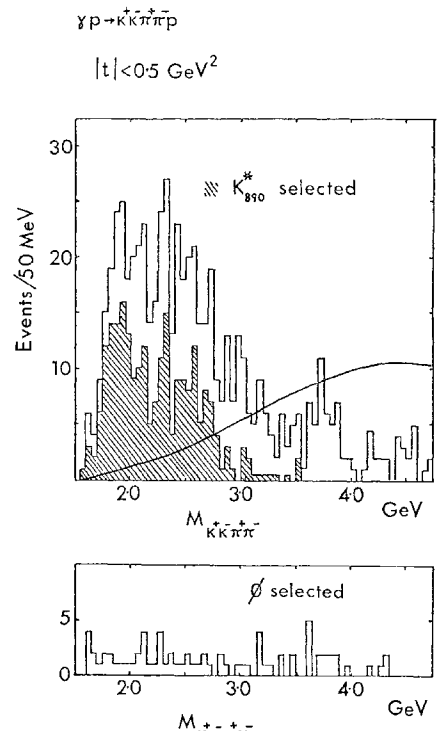


Fig. 3.

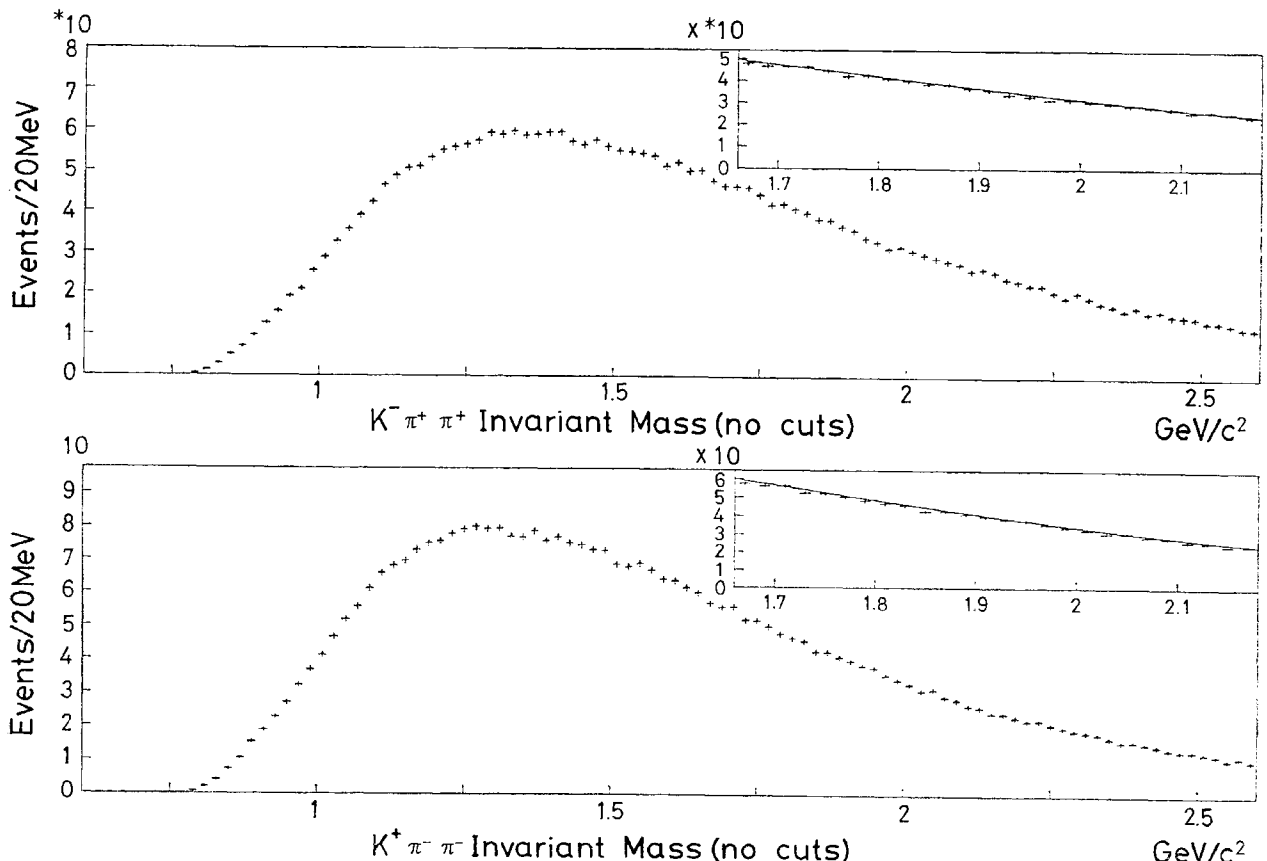


Fig. 4.

similar momentum distributions in each case. Similar values were obtained from the simulation. For the $K\pi\pi$ channels we have taken 76 MeV FWHM.

Mass distributions for $K^\pm\pi^\mp$ and $K^\pm\pi^\mp\pi^\mp$ show no significant peak at the mass of the D . We therefore deduce, for our sensitivity of 60 events/nb, limits on $\sigma \cdot B \cdot \epsilon$ at the 90% confidence level (ϵ is the product of acceptance and efficiency).

Using published values of the branching ratios we obtain upper limits on the inclusive cross sections for D production; these are given in Table I where we have taken the values of $\sigma \cdot B \cdot \epsilon$ and divided by $B \cdot \epsilon$ without taking the errors on B and ϵ into account. The limits range from 0.4 to 1.0 μb .

The interpretation of these data in terms of a total charm production cross-section is strongly model dependent, however since pair production of D -mesons is included in either of the sums $\bar{D}^0 + D^-$, or $D^0 + D^+$ we see that the present limit is about 1.5 μb for the x range accepted.

In order to attempt to obtain a lower limit

Table I. Limits on σ_D .

Decay channel	Upper limit $\sigma \cdot B$	B	σ^*
$D^0 \rightarrow K^+\pi^-$	7 nb	$0.018 \pm .005$	$0.4 \mu\text{b}$
$\bar{D}^0 \rightarrow K^+\pi^-$	19 nb	$0.018 \pm .005$	$1.0 \mu\text{b}$
$D^+ \rightarrow K^-\pi^+\pi^+$	34 nb	0.039 ± 0.010	$0.9 \mu\text{b}$
$D^- \rightarrow K^+\pi^-\pi^-$	21 nb	0.039 ± 0.010	$0.5 \mu\text{b}$

Table II. Limits on σ_D for $p_D/E_\gamma > 0.5$ for D states

Decay Channel	Upper limit $\sigma \cdot B$	B	σ^*
$D^0 \rightarrow K^+\pi^-$	10 nb	0.018 ± 0.005	$0.5 \mu\text{b}$
$D^- \rightarrow K^+\pi^-\pi^-$	10 nb	0.039 ± 0.010	$0.3 \mu\text{b}$

* Column 2 divided by column 3 with no allowance for error on B .

on associated production, we have examined the spectra for D^- and \bar{D}^0 decays in the case where the D has more than half of the incoming photon momentum. The resultant mass plots are shown in Fig. 4 and give the limits in Table II, thus the upper limit on associated production is about 0.8 μb .

PROC. 19th INT. CONF. HIGH ENERGY PHYSICS
TOKYO, 1978

B 4

Hadronic Content of Photons

Presented by D. O. CALDWELL

University of California, Santa Barbara

Using the tagged photon beam we developed at Fermilab, our group has performed three experiments which display the hadronic content of high energy photons. These are measurements of (1) the total photon cross section on hydrogen, to see if there is a rise with energy as is displayed by hadrons; (2) the total photon cross section on nuclei to see from "shadowing" effects the strong interaction of photons; (3) the photoproduction of vector mesons, to compare with π -p and K -p cross sections, via vector-meson-dominance (VMD) and the quark model.

The measurements are difficult because the electromagnetic background is hundreds or even thousands of times larger than the hadronic signal. There is not time to discuss experimental details, but the essential idea is to veto electromagnetic events at small angles (using the equality of the incident photon energy and the downstream electromagnetic energy) and to detect hadrons at larger angles. To avoid missing hadronic events, hadron detectors covered at least 90° in the γ -p center of mass system. The longitudinal spacing of the detector system, which